Materials Chemistry and Physics 119 (2010) 19–29

Contents lists available at ScienceDirect

Materials Chemistry and Physics

journal homepage: www.elsevier.com/locate/matchemphys

Corrosion resistance of Cr(III) conversion treatments applied on electrogalvanised steel and subjected to chloride containing media

C.R. Tomachuk[a], C.I. Elsner[b], A.R. Di Sarli[b,*], O.B. Ferraz[a]

[a] Corrosion and Degradation Division, National Institute of Technology, Av. Venezuela, 82 sala 608, CEP 20081-312, Rio de Janeiro, RJ, Brazil
[b] CIDEPINT: Research and Development Center in Paint Technology (CIC-CCT-CONICET-La Plata), Av. 52 s/n entre 121 y 122, CP B1900AYB, La Plata, Argentina

ARTICLE INFO

Article history:
Received 31 January 2009
Received in revised form 10 June 2009
Accepted 19 July 2009

Keywords:
Interfaces
Corrosion
Electrochemical properties
Coatings
SEM

ABSTRACT

The corrosion resistance of pure zinc coatings can be improved through the application of suitable chemical passivation treatments. Hexavalent chromium compounds have widely been used to formulate conversion layers providing better anticorrosive protection as well as anchorage properties to painting systems. However, taking into account that they are produced using hazardous chemical compounds, the development of alternative and "green" technologies with equivalent protective performance is a paramount purpose of many R&D laboratories working around the world. In the present paper, the corrosion behavior of zinc coatings obtained from free-cyanide alkaline baths and later subjected to a Cr^{3+} based passivation treatment, with and without a sealing treatment, was studied. The experimental work involved electrochemical impedance spectroscopy measurements in 0.5 M NaCl solution, surface microstructural and morphological characterization by electronic microscopy as well as chemical analysis by EDXS. The salt spray test was also performed. The analysis and interpretation of all the data coming from this battery of tests allowed inferring that both the Cr^{3+} based conversion treatment + adequate sealer presented a good corrosion resistance and, therefore, they could be used as neither a polluting nor toxic alternative to the traditional chromate coatings.

1. Introduction

The zinc coatings are employed as active galvanic protection for steel. However, as zinc is an electrochemically high reactive metal, its corrosion rate may also be high indoors but particularly high under outdoor exposure conditions [1]. For this reason, a post-treatment is necessary in order to increase the lifetime of zinc coatings, and with this objective chromates are used in a wide range of industries, including construction, food, automotive, appliances, conversion coating and as a pigment of the primer of painting schemes. The chromatation layer has a number of functions such as acting like anodic inhibitor, forming a passive layer and lowering the zinc dissolution rate. It is also an efficient cathodic inhibitor, lowering the rate of the oxygen reduction reaction on the metal surface and avoiding the formation of blisters [2], i.e., it acts as a corrosion inhibitor, providing excellent protection particularly at defective areas such as crevices or cut edges [3]. Besides, it promotes adhesion between the substrate and the paint. On the other hand, the increasingly stricter environmental legislation all over the world restricts the use of chromate. In the European Community, the use of Cr(VI) compounds, considered a cancer-producing agent, must be withdrawn within a short time, according to the regulations 2002/95/CE and 2000/53/CE related to the electronic/appliances and automotive industries, respectively [4]. A zinc layer itself provides slightly better corrosion resistance than bare steel; therefore, most items coated with zinc by electroplating or hot-dipping are often protected together with another coating system in order to induce a synergistic action. The term conversion coating, as used in the metal-finishing industry, refers to the conversion of a metal surface that can easily accept applied coatings and/or make it more corrosion-resistant [5]. Although the beginning of the chromium-based conversion coatings can be traced back to 1915 [6], the advent of modern-day chromating coatings is recorded from 1945 to the early 1950s [7–9]. They are formed by a chemical or an electrochemical treatment of metal or metallic coatings in solutions containing chromium ions and, usually, other components. The process results in the formation of an amorphous protective coating composed of the substrate, complex chromium compounds, and other components of the processing bath.

In the last 30 years, zinc plating has had remarkable development because of the increasing demand from the automotive industry for coatings with better corrosion resistance. If pure zinc is used, such resistance can be improved by applying suitable

* Corresponding author. Tel.: +54 221 483 1141/44; fax: +54 221 427 1537.
E-mail addresses: celia@br.surtec.com (C.R. Tomachuk), direccion@cidepint.gov.ar, ardisarli@ciudad.com.ar (A.R. Di Sarli).

0254-0584/$ – see front matter © 2009 Elsevier B.V. All rights reserved.
doi:10.1016/j.matchemphys.2009.07.041

Table 1
Samples and description of Cr^{6+} free makeup coatings.

Sample	Description
TA	Zn + chromatizing process free of Cr^{6+} and complexing agents (Tridur Azul 3HPC®)
TAC	**TA + S1** (treatment with corrosion inhibitors and a product based on silica stabilized with organic additives (Corrosil Plus 501 N®))
Z80	Zn + chromatizing process free of Cr^{6+} and oxidizing agents (SurTech 680®)
Z805	**Z80 + S3** (treatment with a Cr^{6+} free liquid dispersion and mineral particles (SurTech 555S®))
Z806	**Z80 + S2** (treatment free of Cr^{6+} and oxidant products (SurTech 662®))
Z66	Zn + passivation process free of Cr^{6+}, oxidative agents and fluorine ions (SurTech 666®)
Z665	**Z66 + S3** (treatment with a Cr^{6+} free liquid dispersion with mineral particles (SurTech 555S®))
Z666	**Z66 + S2** (treatment free of Cr^{6+} and oxidant products (SurTech 662®))

chemical passivation treatments whose baths contain additives such as fluoride, sulfate or acetate to produce thicker conversion layers as well as higher painting system adhesion. These layers protect the zinc coating by acting as a physical barrier to the inducing corrosion species (water, oxygen and ions), and corrosion inhibitor. Furthermore, when scratched or mechanically damaged, enough water is absorbed by the layer to swell and mend the damaged areas (self-healing effect) [10].

The trivalent chrome (Cr^{3+}) conversion coating technology was commercially introduced in the late 1980s as an earlier attempt to replace the carcinogenic hexavalent chrome from as many metal-finishing processes as possible.

Many investigations and valuable results related with chromate coatings have been reported, but the protective mechanism of the chromate coatings is still not fully known [11–14]. Consequently, extensive fundamental research is still needed in order to elucidate the protective mechanism of the chromate conversion coating and, from this fact, to find effective but non-toxic and environmentally friendly alternatives.

The main purpose of the present work was to study a non-toxic and environmentally friendly conversion treatment, which can successfully replace the Cr^{6+} based one. In order to do this, it was evaluated the corrosion behavior of electrogalvanised steel panels covered with alternative Cr^{6+} free treatments and then immersed in 0.5 M NaCl solution by using AC and DC electrochemical techniques. Replicates of these panels were subjected to the salt fog chamber test. The analysis of the surface morphology and chemical composition was also performed.

2. Experimental details

2.1. Samples preparation

AISI 1010 steel sheets (7.5 cm × 10 cm × 0.4 cm) were industrially electrogalvanised using a cyanide-free alkaline bath containing Zn^{2+} 10–12 g L^{-1}, NaOH 130–140 g L^{-1}, commercially available additives, and the following operative conditions: temperature 25 °C and cathodic current density 2 A dm^{-2}. Immediately after finishing the zinc deposition step, each sample was coated with the Cr^{3+} based makeup described in Table 1 according to the operating conditions recommended by the supplier (Table 2). At the end of this step, samples were again rinsed with deionized water, and then dried.

2.2. Thickness measurements

The coating thickness was measured with the magnetic inductive method using the Helmut Fischer equipment DUALSCOPE MP4 according to ASTM B499: 1996 (2002) standard. To evaluate the conversion layer thickness, the samples were cut and their cross-sections observed with scanning electron microscopy (SEM).

2.3. Quali-quantitative chemical analyses and morphology

Morphological analyses of coatings were conducted by means of SEM with a LEO 440i microscope, while their composition was obtained using Energy Dispersive X-Ray Spectroscopy (EDXS).

2.4. Electrochemical and corrosion behavior

2.4.1. Corrosion potential and EIS measurements

The electrochemical cell consisted of a classic three-electrode arrangement; where the counter electrode was a platinum sheet, the reference one a saturated calomel electrode (SCE = +0.244 V vs. NHE) and the working electrode each coated steel sample with a defined area of 15.9 cm^2. All measurements were performed at a constant room temperature (22 ± 3 °C) in 0.5 M NaCl solution.

Impedance spectra in the frequency range 10^{-2} Hz < f < 10^5 Hz were performed in the potentiostatic mode at the open circuit potential, as a function of the exposure time in the 0.5 M NaCl solution, using a Solartron 1255 Frequency Response Analyzer (FRA) coupled to a Solartron 1286 electrochemical interface (EI) and controlled by the ZPlot® program. A sinusoidal signal with amplitude of 15 mV peak to peak was applied and 10 points per decade were registered. The corrosion behavior was analyzed until white corrosion products could be seen by the naked eye on the samples' surface. The experimental spectra were fitted and interpreted based on equivalent electrical circuits using the software (EQUIVCRT) developed by Boukamp [15]. On the triplicate specimens of each sample, all impedance measurements were performed with the electrochemical cell inside the Faraday's cage to reduce as much as possible any external electromagnetic signal able to disturb the studied system. The integrity of samples was checked by measuring the corrosion potential after each test to confirm that their change from the initial value was less than ±0.005 V.

2.4.2. Salt spray test

Triplicate specimens of each sample were tested in salt spray chamber in accordance with ASTM B117: 2002 standard. The surface percentage covered with red rust was evaluated at various exposure times.

Table 2
Coating films and operating conditions.

Parameter	Sample							
	TA	**TAC (TA + S1)**	**Z66**	**Z666 (Z66 + S2)**	**Z665 (Z66 + S3)**	**Z80**	**Z806 (Z80 + S2)**	**Z805 (Z80 + S3)**
Makeup + zinc coating (% v/v)								
Cr	0.02	0.04	0.05	0.02	0.04	0.14	0.17	0.15
Zn	Rest	Rest	Rest	Rest	Rest	Rest	Rest	Rest
Si	–	1.19	–	0.68	0.58	–	0.95	0.44
Co	–	–	–	–	–	0.02	–	–
pH	1.6–2.0	8.0–9.0	1.7–2.2	7.0–8.5	9.0–9.5	1.6–2.1	7.0–8.5	9.0–9.5
Bath temperature (°C)	22	25	25	25	25	60	25	25
Immersion time (s)	30	15	30	10	20	60	10	20
Drying temperature (°C)	60	60	25	70	70–120	25	70	70–120
Agitation	Mechanical							
Activation	0.5% HNO_3 solution for 10 s and then rinsed in deionized water							
Film color	Blue	Blue	Blue	Blue	Blue	Green iridescent	Green	Green
Total coating thickness (μm)	11.8 ± 0.86	10.7 ± 0.93	8.4 ± 0.43	7.8 ± 0.37	8.2 ± 0.35	10.4 ± 1.43	10.3 ± 0.77	9.1 ± 0.28

3. Results and discussion

The identification symbol, chemical composition and overall coating thickness of the tested samples are reported in Table 1. In it, the dispersion of the average coating tickness values was atributted not only to measurement errors but mainly on the fact that both, the galvanic coating and the conversion layer, were built up under operation conditions in a continuous galvanising line, where this type of dispersion commonly occurs. On the other hand, although information related with the specific thickness of the passivated layers could not be obtained, it was possible to observe that the films were continuous throughout the entire surface.

The table also shows that results provided by the surface coating analyses made with EDXS revealed the presence of mainly Cr, Si (when the sealant was applied) and Zn as components of the makeup and the underlying coating, respectively. In some cases, the sealing treatments changed the coating chromium content probably due to osmotic phenomena (increasing) or the fact that some chromium ions could be lost (decreasing) [16]. Cobalt ions detected in sample **Z80** suggest an improvement of its corrosion resistance [17]. However, in samples **Z805** and **Z806** cobalt was not detected as it may have been lost during the sealing process according to what was previously remarked in reference to chromium ions. In order to explain that experimental result, it is presumed that the cobalt contained in the conversion layer was removed by the F^- ions coming from the sealant, and replaced by Cr^{3+} ions, which also form part of the sealant composition.

3.1. Morphology

Fig. 1 shows that the conversion layer was distributed on the entire surface and that, except in preferentially etched zones, it did not present the typical network of cracks characteristic of chromate coatings. Such a result suggests that an individual orientation of the zinc crystals influences the conversion layer structure [18].

Sample **TA** (Fig. 1a) showed a roughed but without microporosity surface. The marks on the surface were attributed to an incorrect handling during transportation. The same conversion treatment covered with a sealer layer (sample **TAC**, Fig. 1b) presented an increase of the surface roughness as the main difference.

Samples **Z66** (Fig. 1c) and **TA** did not exhibit significant morphological differences because the applied conversion layer formulation was quite similar (see Table 1). Fig. 1d and e shows the surface morphology of samples **Z666** and **Z665**, respectively. The sealing treatment 2 (sample **Z666**) proved to be ineffective due to fissures and microporosities formed on the passivated layer. On the other hand, sample **Z665** using the sealant 3 exhibited small spherical shaped particles distributed on the surface, which had a strong tendency to agglomerate forming filaments of inorganic particle groups.

The surface of sample **Z80** (Fig. 1f) presented an irregular size growth, and the morphology of samples **Z806** (Fig. 1g) and **Z805** (Fig. 1h) was similar to that of samples **Z666** and **Z665** (Fig. 1d and e, respectively). This fact may suggest that the sealed coating layer was not influenced by the conversion treatment formulation.

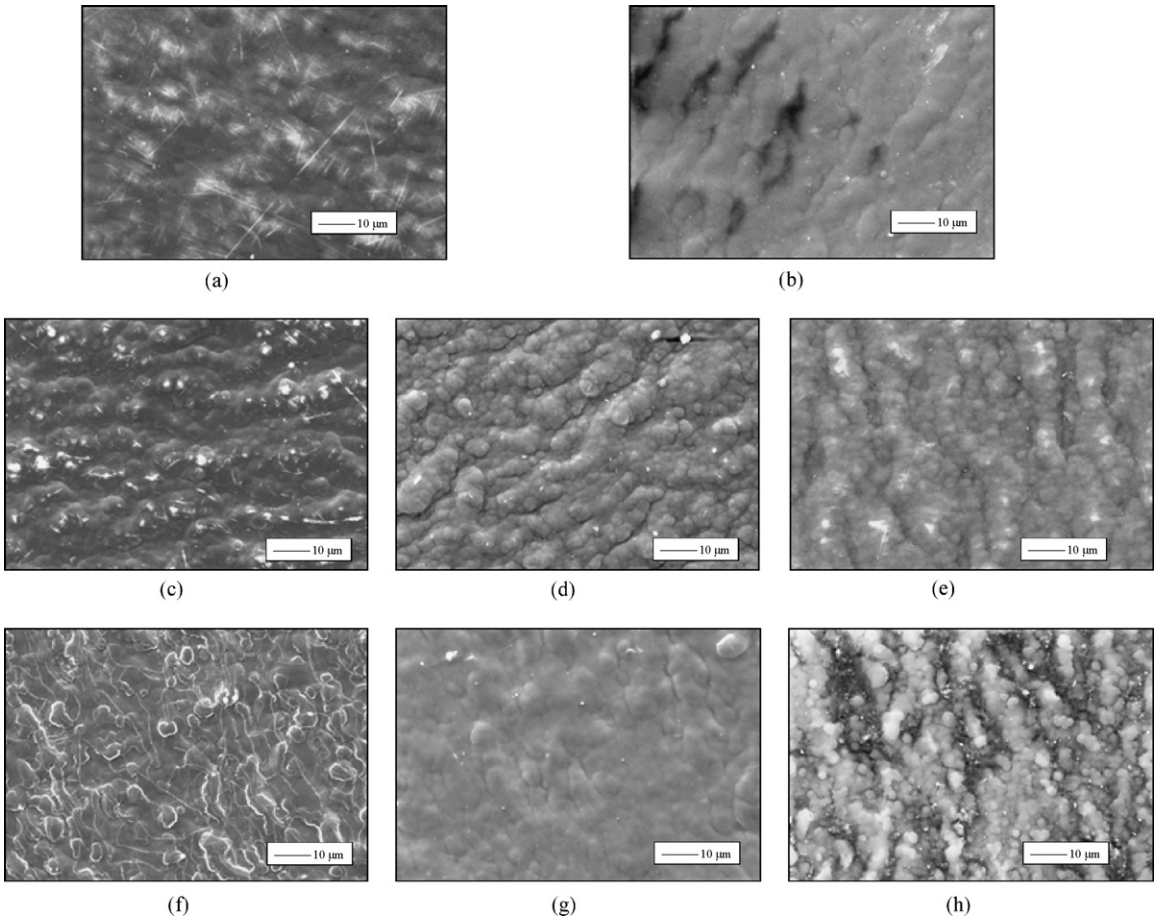

Fig. 1. Microstructure of the tested coatings. (a) **TA**; (b) **TAC**; (c) **Z66**; (d) **Z666**; (e) **Z665**; (f) **Z80**; (g) **Z806**; and (h) **Z805**.

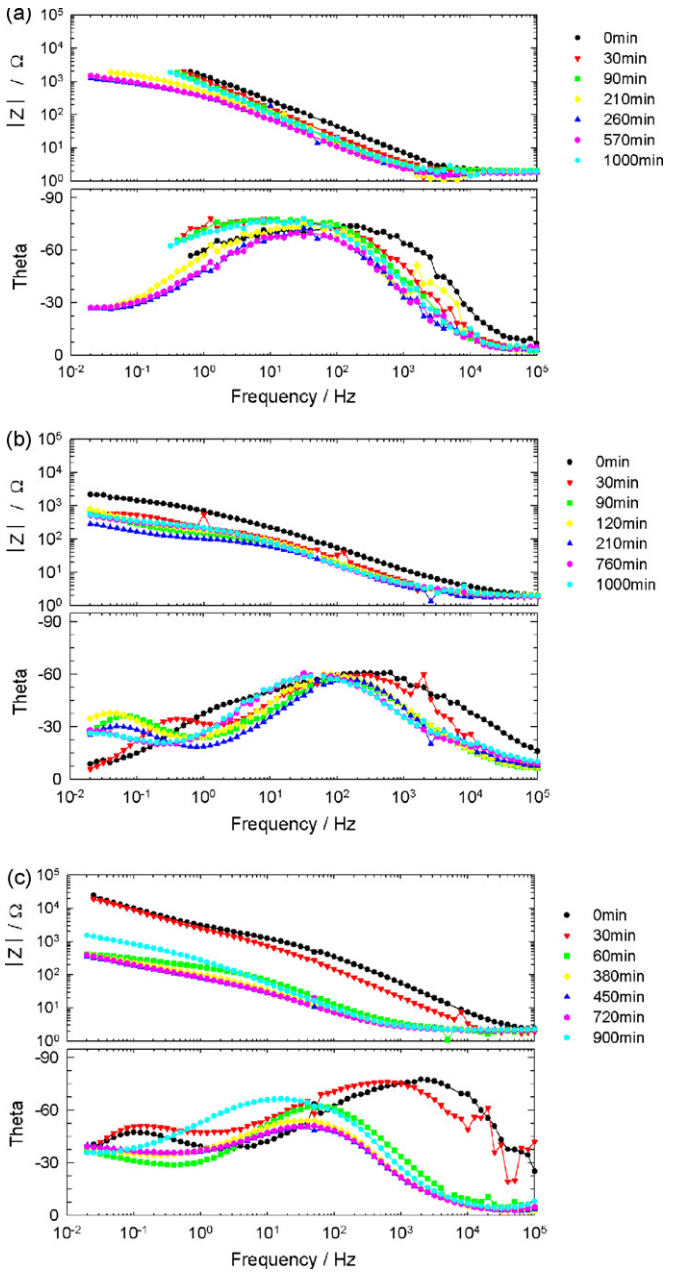

Fig. 2. Bode plots showing the time dependence of the **TA** (a), **Z66** (b) and **Z80** (c) samples impedance at short immersion periods in 0.5 M NaCl solution.

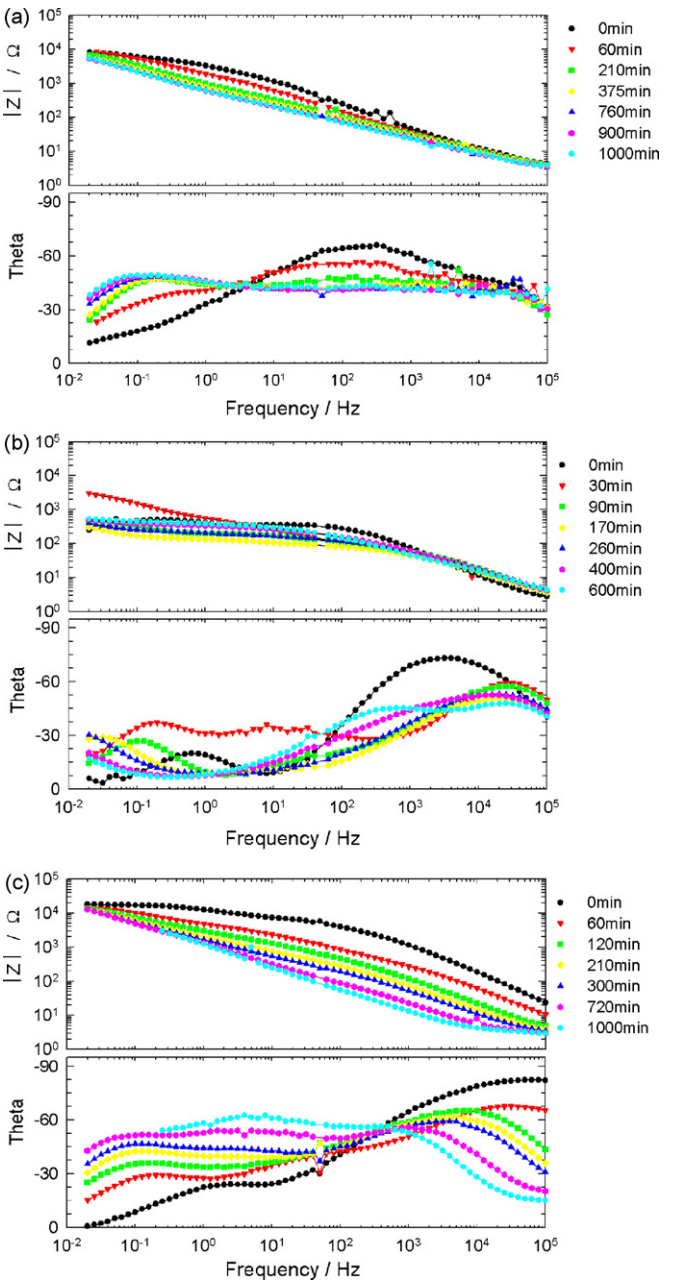

Fig. 3. Bode plots showing the time dependence of the **TAC** (a), **Z665** (b) and **Z805** (c) samples impedance at short immersion periods in 0.5 M NaCl solution.

3.2. Electrochemical behavior

3.2.1. EIS measurements

Results obtained by EIS measurements allow to improve the insight related with the electrochemical characteristics of the tested conversion treatments. It is important to emphasize that when the conversion layer is used as the outermost one in the coating system, electrochemical interactions between this layer and its surrounding medium start just after getting in contact, particularly if the medium is a saline aqueous solution. In such circumstances, the chromium content in the conversion layer plays an important role either providing a barrier resistance to the corrosion-inducing species diffusion towards the underlying zinc or inhibiting the oxygen reduction reaction. The effectiveness of these actions can be improved through the sealing treatment. However, as each conversion layer behavior depends upon its composition, desirable protective properties are only obtained if the adequate sealant is used.

3.2.1.1. Bode plots.

3.2.1.1.1. Short immersion times.

3.2.1.1.1.1. Samples without sealing treatment. Experimental results obtained with the eight types of tested samples exposed to 0.5 M NaCl solution clearly proved that the zinc corrosion process started just after immersion.

Figs. 2–4 show the Bode plots of the electrochemical impedance evolution for short immersion times (less than 24 h). At first glance, a qualitative comparison among the coating corrosion resistance can be accomplished from a simple visual analysis of the time dependence $|Z|$ and phase angle (Theta) values [19].

In Fig. 2a it can be observed that, at low frequencies, the sample **TA**'s $|Z|$ values decreased almost one order of magnitude before

24 h immersion, suggesting the presence of an increasing activity within the coating layer and at the metal/coating interface. This behavior was confirmed by the angle phase (Theta) evolution where the maximum value not only shifted towards lower frequencies but also decreased indicating the loss of part of the coating dielectric capacity (i.e. its isolating effect).

For sample **Z66** (Fig. 2b) the decrease of impedance values at medium and low frequencies suggested a fast corrosion-inducing species permeation up to the metal/coating interface. This fact was confirmed by the appearance of a well-defined second time constant at low frequency, which was easily visible in the phase angle plot. The slight increase of $|Z|$ and Theta values after the corrosive attack was attributed to the corrosion products gathered within the pores and/or other coating defects, which improved the coating barrier protection.

With regard to sample **Z80** (Fig. 2c) it can be seen that at low frequencies it exhibited higher initial $|Z|$ values than samples **Z66** and **TA**. This behavior was in agreement with that inferred from polarization curve measurements and confirmed that this conversion treatment yielded a better barrier effect due to the more compact structure of the coating thickness. After 60 min exposure, the $|Z|$ values at medium and low frequencies decreased about one order of magnitude and remained close to $10^3\ \Omega$, suggesting an electrochemically active interface. At lower frequencies, the impedance related to the conversion coating properties showed a slight increase, which was ascribed to an improvement of the coating protective properties; however, as it will be demonstrated in the next paragraphs, it was not enough to prevent the substrate corrosion at longer immersion periods. This type of behavior could be explained assuming that initially the loose corrosion products tended to become more compact, but as time elapsed, part of them diffuse towards the electrolyte contributing to diminish the coating

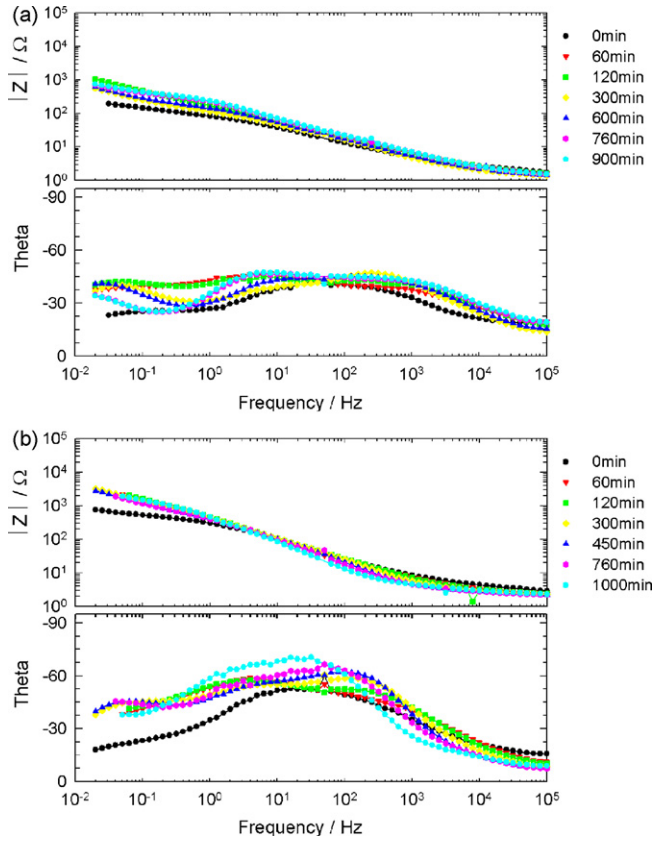

Fig. 4. Bode plots showing the time dependence of the **Z666** (a) and **Z806** (b) samples impedance at short immersion periods in 0.5 M NaCl solution.

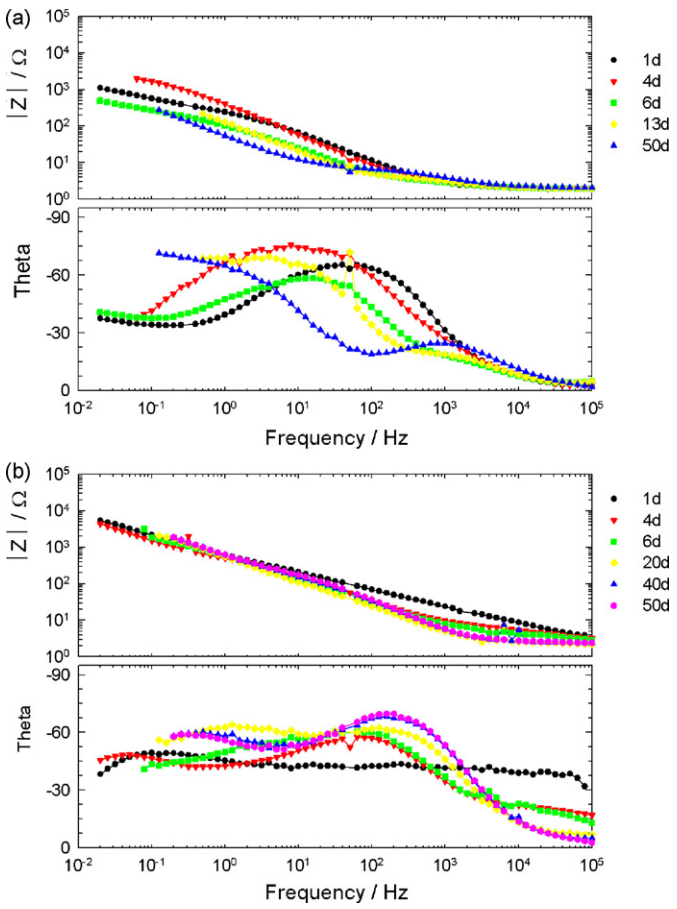

Fig. 5. Bode plots showing the time dependence of the **TA** (a) and **TAC** (b) samples impedance at long immersion periods in 0.5 M NaCl solution.

resistive and capacitive properties. In spite of this, changes underwent by the conversion layer had no very significant effect on the corrosion behavior of the total coating probably due to the cobalt content.

From a qualitative point of view, it can be presumed that sample **Z80** showed higher degradation resistance than other analyzed alternative treatments and, as a possible consequence that also provided a better corrosion protection to the metallic substrate.

3.2.1.1.1.2. Samples with sealing treatment. By analyzing samples with sealing treatment, sample **TAC** (Fig. 3a) showed a less degradation rate than **TA**, which suggested a more effective barrier acting to diminish the corrosion rate during the exposure to the aggressive solution. This result was confirmed by the increasing trend showed by the phase angle evolution at medium and low frequencies, i.e., the development of more resistive pathways to the corrosive species towards the zinc substrate.

In spite of having identical sealant, samples **Z665** and **Z805** (Fig. 3b and c) showed different behavior. Initially, the $|Z|$ values of sample **Z665** were lower than those of **Z805**; however, in both cases the values suggested high electrochemical activity at the zinc/conversion layer interface. At the lowest frequencies, the $|Z|$ values for sample **Z805** remained unchanged during all the immersion time, and close to $10^4\ \Omega$ probably due to an improvement of the anticorrosive properties provided by both the higher chromium content and the sealant 3 presences in this conversion layer. For sample **Z665**, these values ranged between 10^2 and $10^3\ \Omega$. At high and medium frequencies, changes observed for sample **Z805** indicated continuous fluctuations of the resistive and capacitive components of these samples impedance. However, sample **Z665** did not show variations along the immersion time.

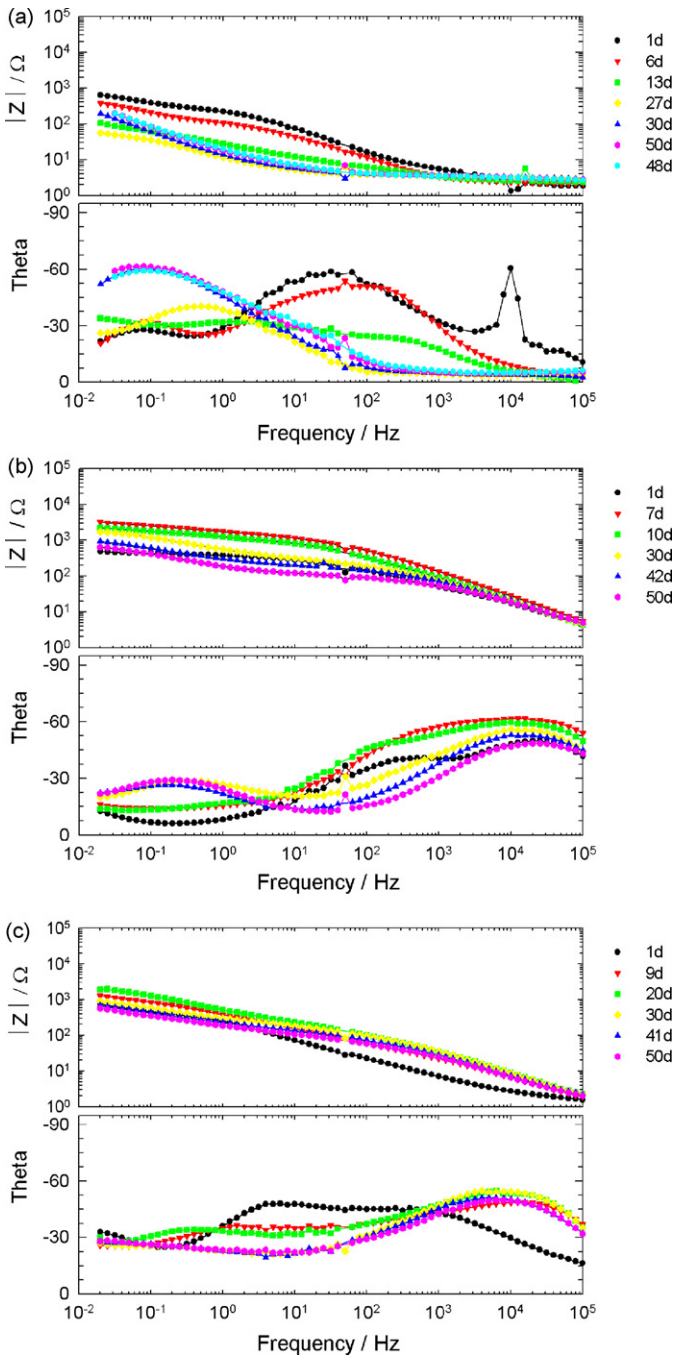

Fig. 6. Bode plots showing the time dependence of the **Z66** (a), **Z665** (b) and **Z666** (c) samples impedance at long immersion periods in 0.5 M NaCl solution.

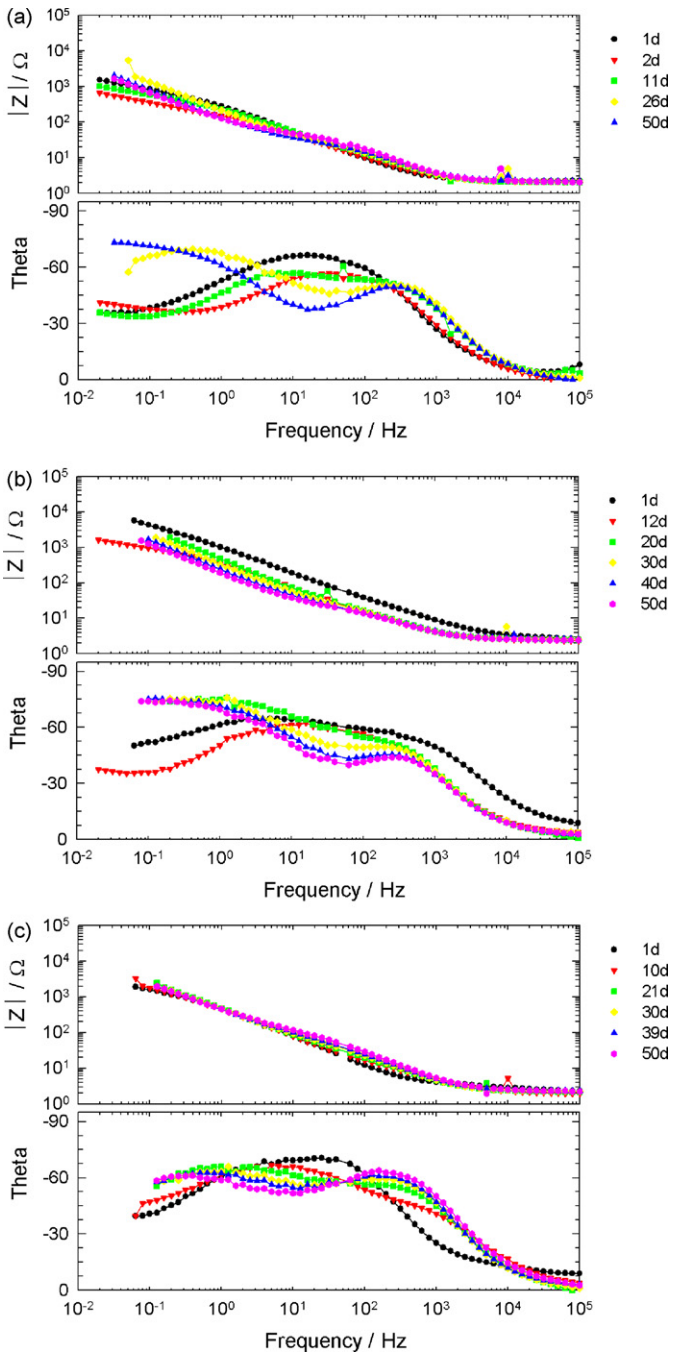

Fig. 7. Bode plots showing the time dependence of the **Z80** (a), **Z805** (b) and **Z806** (c) samples impedance at long immersion periods in 0.5 M NaCl solution.

For samples **Z666** (Fig. 4a) and **Z806** (Fig. 4b), the $|Z|$ and phase angle values showed almost no significant changes during the first immersion day. The sample **Z666** behavior, being similar to **Z66**, suggested that the sealing treatment did not improve its corrosion resistance. This fact could be due to the fissures observed on their respective surfaces (Fig. 1c and d). On the other hand, the initial response of sample **Z806** was worse than that of **Z80**, that is to say, the electrochemical reactivity was higher; however, after 60 min immersion, the impedance spectra of both were very similar (Figs. 4b and 2c, respectively). Such a difference could be attributed to the fact that the presence of a very small concentration of Co in sample **Z80** led to a short induction time for the corrosion attack initiation.

3.2.1.1.2. Long immersion times.

3.2.1.1.2.1. Samples either without or with sealing treatment. In Fig. 5a and b, it can be seen that long immersion in 0.5 M NaCl solution promoted no significant changes in the $|Z|$ values of sample **TA**, but for **TAC** they were nearly one order of magnitude

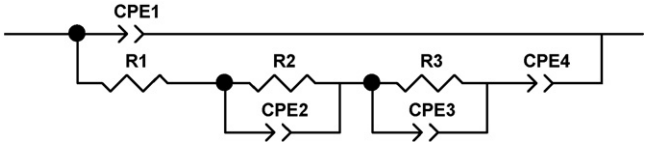

Fig. 8. Equivalent circuit model used for fitting tested samples.

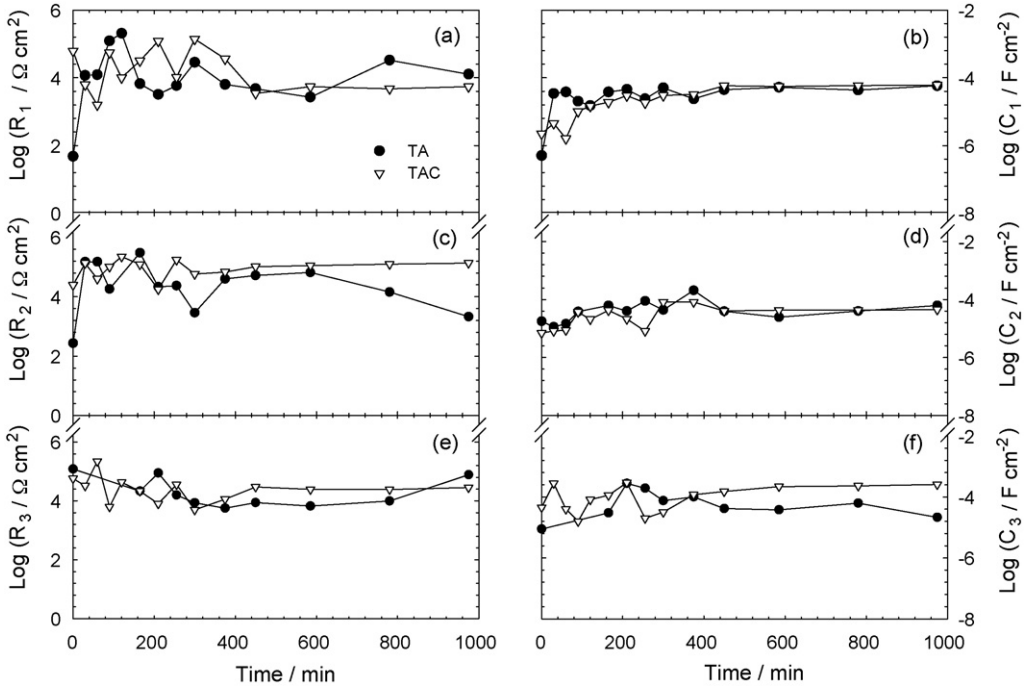

Fig. 9. Evolution of (a) $\log R_1$; (b) $\log C_1$; (c) $\log R_2$; (d) $\log C_2$; (e) $\log R_3$; and (f) $\log C_3$ parameters of samples **TA** and **TAC** at short exposure times in 0.5 M NaCl solution.

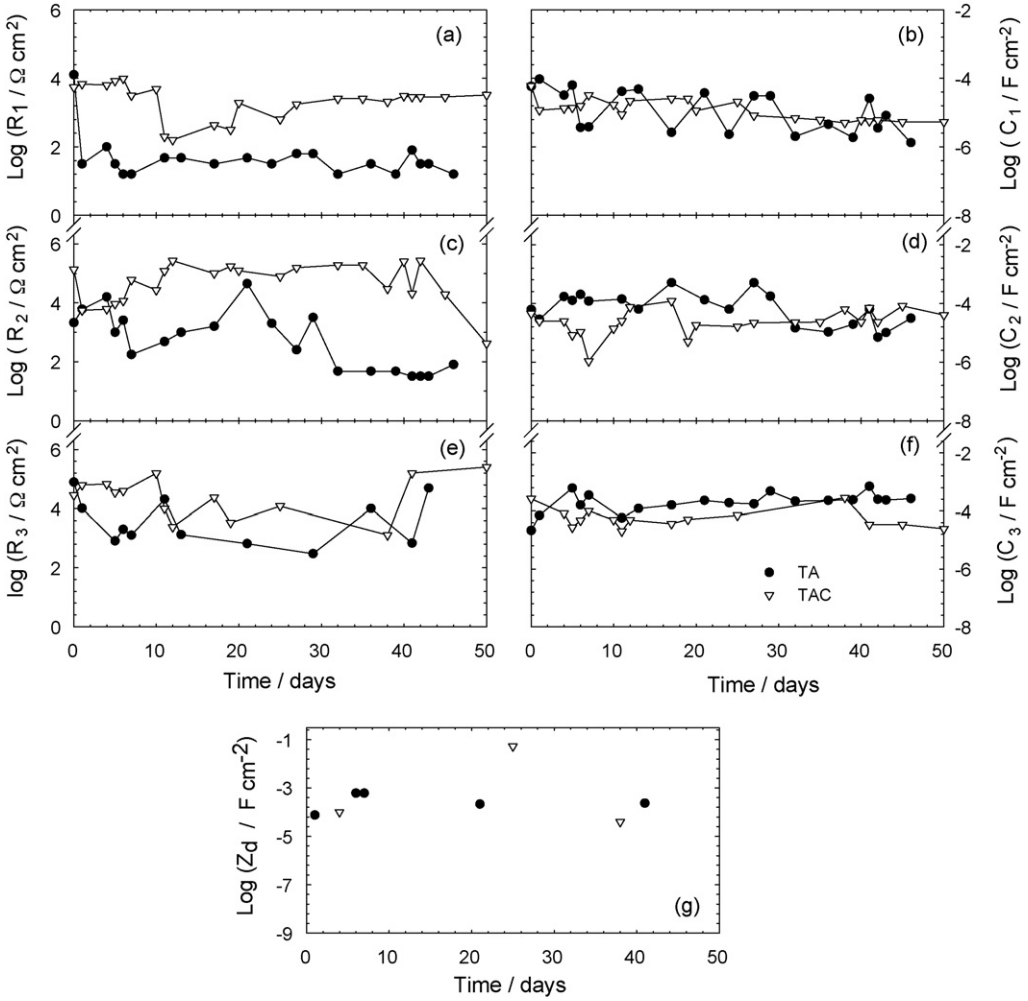

Fig. 10. Evolution of (a) $\log R_1$; (b) $\log C_1$; (c) $\log R_2$; (d) $\log C_2$; (e) $\log R_3$; (f) $\log C_3$; and (g) $\log Z_d$ parameters of samples **TA** and **TAC** at long exposure times in 0.5 M NaCl solution.

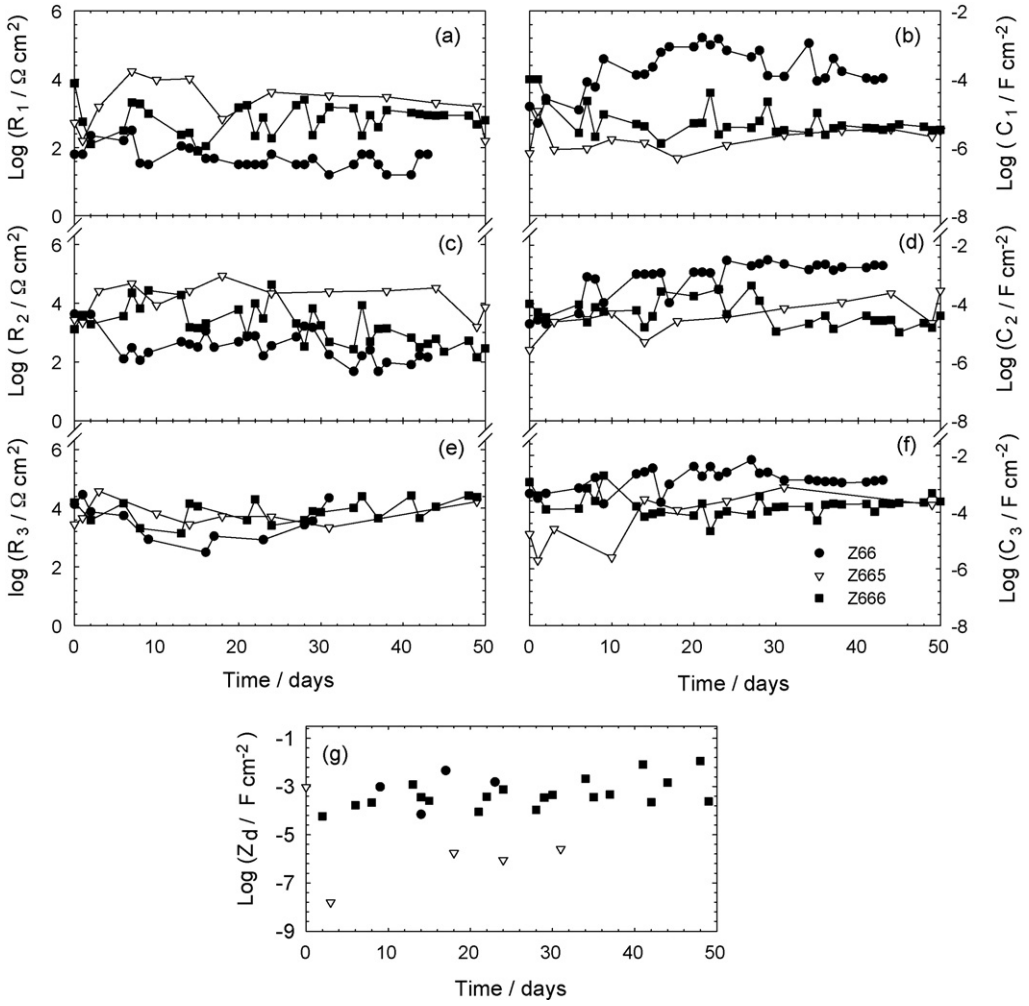

Fig. 11. Evolution of (a) $\log R_1$; (b) $\log C_1$; (c) $\log R_2$; (d) $\log C_2$; (e) $\log R_3$; (f) $\log C_3$; and (g) $\log Z_d$ parameters of samples **Z66**, **Z665** and **Z666** at long exposure times in 0.5 M NaCl solution.

less than that measured at short times. Besides, by comparing the performance of both samples during the two exposure periods, greater and better-defined changes in the phase angle plots were observed. Therefore, from these results it could be inferred that the sealant did not improve the coating protective performance.

With regard to the time dependence of the impedance module and the angle phase of samples **Z66**, **Z665** and **Z666** (Fig. 6a–c), and **Z80**, **Z805** and **Z806** (Fig. 7a–c) submerged in the same solution, a similar response to that described in the above paragraph was found. That is to say, independently of the overall coating composition, the main variations along the frequency range swept suggested that there was a poor barrier resistance as well as evidence of certain electrochemical activity at the conversion treatment/zinc interface.

3.2.1.2. Impedance data deconvolution. One of the most important difficulties for analyzing the electrochemical impedance data from the impedance spectra deconvolution is, in general, to find at least one electrical equivalent circuit model whose resistive and capacitive elements can be associated to the physicochemical processes taking place in reactive and/or complex interfaces. In this sense, the dynamic character of the electrochemical reactions occurring on the coated surface as well as at the bottom of its defects makes that the impedance spectra of conversion layer/electrogalvanised steel/0.5 M NaCl solution systems change the whole immersion time. A fairly good description of their impedance data evolution could be obtained in terms of the transfer function analysis using the non-linear fit routines developed by Boukamp [15]. However, because of the reactive and complex nature of the processes taking place in the tested systems, for describing their time exposure dependence was necessary to perform a preliminary and long series of comparative proofs until the "more probable transfer function and, therefore, equivalent circuit model able to fit satisfactorily the obtained impedance spectra" [15], was found (Fig. 8). In it, the first time constant (R_1·CPE_1) appearing at higher frequencies represents the resistance to the ionic flux (R_1) and the dielectric capacitance (CPE_1) of the conversion layer. As the frequency values diminished, and taking into account that the permeating and corrosion-inducing chemicals (water, oxygen and ionic species) reach the electrochemically active areas of the substrate through the coating defects characterized by R_1, it is reasonable to assume that the corrosion process developing at the zinc surface should be placed in series with R_1. The R_2 and CPE_2 parameters account for the charge transfer resistance and the electrochemical double layer capacitance of the corrosion process. Due to the zinc dissolution, corrosion products accumulate at the bottom of the pores. Their contribution to the system impedance is characterized by the R_3 and CPE_3 parameters [20–23]. The diffusion component Z_d obtained at certain exposure times was associated with an oxygen diffusion-controlled reaction usually found in zinc corrosion [24,25].

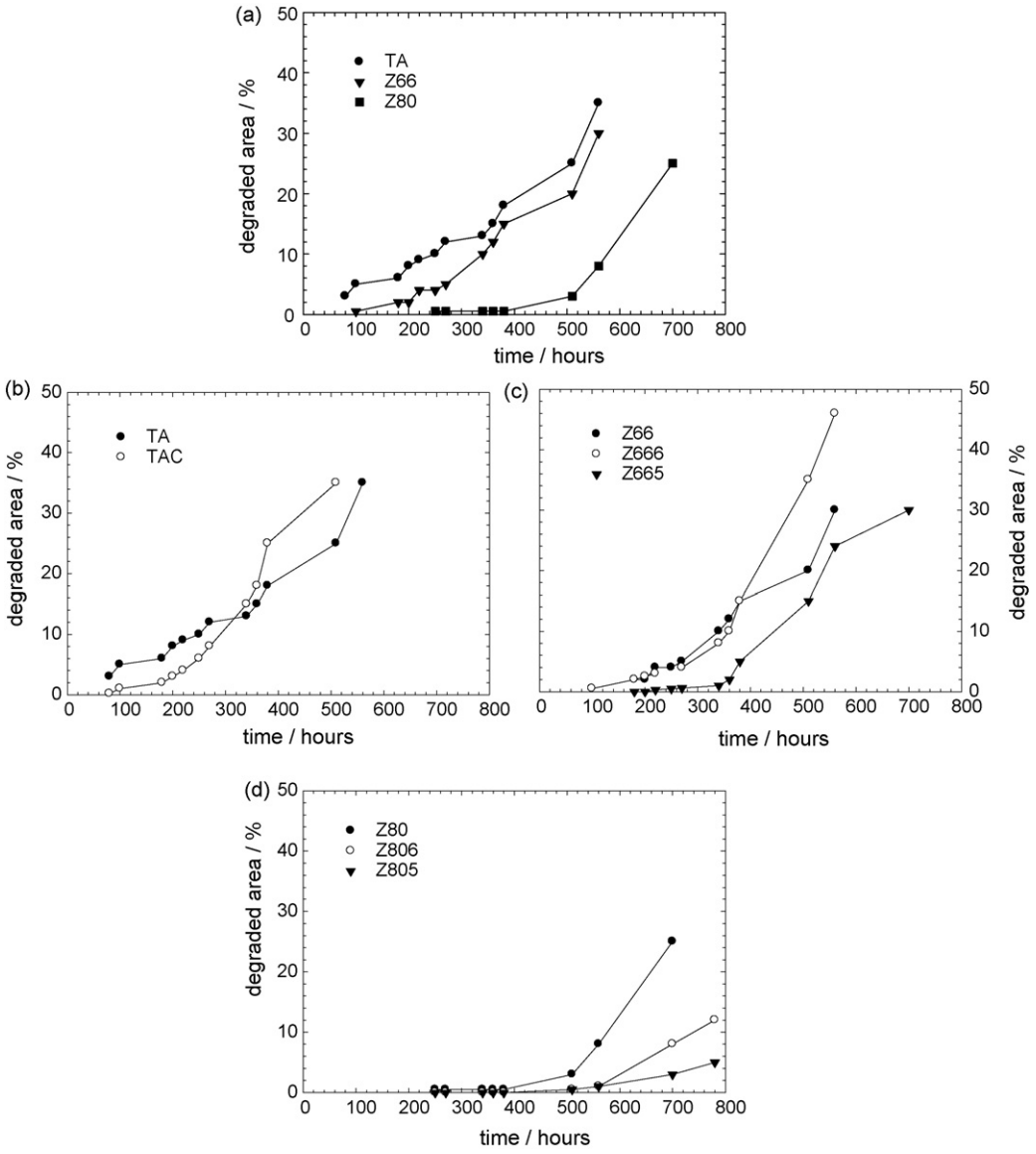

Fig. 12. Surface degradation as a function of the exposure time in the salt spray chamber.

All the time constants exhibited some Cole–Cole type dispersion which had the corresponding n_i parameter, being $0 < n_i \leq 1$. Furthermore, distortions observed in those resistive–capacitive contributions indicate a deviation from the theoretical models in terms of a time constant distribution. This is due to lateral penetration of the electrolyte at the metal/coating interface (usually started at the base of intrinsic or artificial coating defects), to underlying metallic surface heterogeneity (topological, chemical composition and surface energy) and/or to diffusion processes that could take place along the test. Since all these factors may cause the impedance/frequency relationship to be non-linear, they are taken into consideration by replacing one or more capacitive components (C_i) of the equivalent circuit transfer function by the corresponding constant phase element (CPE_i), for which the impedance may be expressed as [26,27]:

$$Z = \frac{(j\omega)^{-n}}{Y_0}$$

where

$Z(\omega) \Rightarrow$ impedance of the CPE ($Z = Z' + jZ''$) (Ω);
$j \Rightarrow$ imaginary number ($j^2 = -1$);
$\omega \Rightarrow$ angular frequency (rad);
$n \Rightarrow$ CPE power ($n = \alpha/(\pi/2)$);
$\alpha \Rightarrow$ constant phase angle of the CPE (rad);
$Y_0 \Rightarrow$ part of the CPE independent of the frequency (Ω^{-1}).

When difficulties in providing an accurate physical description of the occurred processes were found a standard deviation (χ^2) $\leq 5 \times 10^{-4}$ was used as final criterion by considering that the smaller this value, the closer the fit to the experimental data [15]. In the present work, the fitting process was mainly performed using the phase constant element (CPE_i) instead of the dielectric capacitance C_i. However, this last parameter was used in the following plots in order to facilitate the results visualization and interpretation.

The $R_1, C_1, R_2, C_2, R_3, C_3$ and Z_d parameter values estimated from the impedance spectra fitting analysis for short and long exposure times are respectively reported in Figs. 9a–f, 10a–g and 11a–g. As a result of the dynamic changes suffered throughout the test by the heterogeneous composition and morphology of both the substrate surface and the zinc corrosion products, a high variation of the time

constant values associated to the interfacial processes evolution was observed.

3.2.1.3. Time dependence of the impedance resistive and capacitive components.

3.2.1.3.1. Short exposure time. As an example of the gathered experimental results, Fig. 9a–f shows the electrical and electrochemical parameter values obtained from applying the equivalent circuit model to impedance data corresponding to samples **TA** and **TAC**. Therein, it can be seen that both samples provided quantitatively similar oscillating resistive–capacitive time dependence. Despite the fact that the magnitude of these parameters differs, the electrochemical performance of samples **Z80** and **Z66**, either sealed or not, was similar although these showed the appearance of a diffusion component at different immersion times. It is important to point out that, independently of the conversion layer structure and composition, the zinc electrochemical reactivity was very high in this medium. Regarding this, the dynamic behavior of the processes taking place at this interface is reflected by the changing value of the parameters associated to these processes, by the number of time constants (R_iC_i) feasible to be deconvoluted, and by the rate-determining step (rds) of the zinc dissolution reaction. In samples **TA** and **TAC**, the rds was always under active control, while in the rest changed from active to diffusion or vice versa. Such performance may be explained assuming that the protection afforded by the conversion layer in samples **TA** and **TAC** was less effective because their coating structure and higher roughness left unprotected large areas of the underlying zinc substrate.

3.2.1.3.2. Long exposure time. With regard to the barrier property provided by the conversion layer, Fig. 10a–g shows that the R_1 values of sample **TAC** were one to two orders of magnitude larger than those of **TA**. This fact was ascribed to the blockage of pores and defects of that layer provided by the sealing treatment. This improvement was accompanied by also increasing values of the charge transfer resistance (R_2) – i.e., lower corrosion rate – and the resistive contribution (R_3) of the corrosion products coming from the zinc dissolution. Again, the rds dependence on the exposure time fluctuated between active, mass transport and mix that is why, in some cases, an overlapping of their associated time constants took place.

On the other hand, the samples **Z66**, **Z665** and **Z666** response (Fig. 11a–g) showed that probably due to their thinner coating layer all of them presented changes from active to diffusion-controlled zinc dissolution reaction at different immersion times. Such behavior was attributed to the dynamic nature of each tested interface, which took place at the same time, or almost, in certain areas. Due to that, the localized corrosion was inhibited by the blocking action of the corrosion products, but it started in other places where the protection was weaker. This mechanism can repeat endlessly along the test until the overall protection disappears and bare steel is exposed. On the other hand, samples **Z80**, **Z805** and **Z806** did not present significant changes or diffusion processes during the test. This may be indicating that their conversion layer was more effective at inhibiting the anodic (zinc corrosion) than the cathodic (oxygen reduction) reactions. Since the gathered corrosion products were not enough for delaying the oxygen transport towards the cathodic areas, it is also reasonable to think that they may have contributed to prevent the oxygen reduction from being the rds.

3.3. Salt spray test

The test was cut off just after red corrosion products were detected on the surface at naked eye. It is important to note that the coating passivation effect is strongly dependent on the application parameters, the thicker the layer the higher the corrosion protection.

Fig. 12a–d shows the surface degradation vs. time during the salt spray exposure of the samples with and without sealing treatment. In Fig. 12a it can be seen that superficial degradation of sample **TA** started after 76 h exposure while for **Z66** and **Z80** this occurred after 100 and 240 h, respectively. Samples **TA** and **Z66** had similar trend to surface degradation. This result is in agreement with electrochemical measurements and could be associated to the less chromium content in the conversion layer.

Fig. 12b–d illustrates that among the sealed samples, the **TAC** showed the earlier degradation followed by **Z666**, **Z665**, **Z806** and **Z805**. Besides, by comparing samples treated with either sealant 2 or 3, it can be observed that those using sealant 3 always afforded higher anticorrosive protection confirming results obtained from electrochemical measurements.

4. Conclusions

This research work included three conversion layers, either with or without sealing treatments, applied on electrogalvanised steel. From their experimental results, some conclusions with regard to their corrosiveness in environments containing relatively high chloride ions concentration could be drawn:

- The more uniform and compact coatings showed the lower corrosion rates.
- By combining adequate sealant composition, conversion layer thickness (higher barrier resistance) and their Cr(III) contents (corrosion inhibiting effect) it is possible to improve the corrosion behavior of alternative pre-treatments; therefore, a very well designed system could be used as non-pollutant or non-toxic. In this sense, it is important to emphasize that suppliers of commercial steel coated sheets built up in a continuous line should subject them to strong quality tests in order to avoid the high amount of surface defects found along the present research.
- The studied conversion treatments provide interesting insights related with this topic but other experiments need to be performed for evaluating other alternatives to the traditional and highly effective Cr(VI) based conversion treatment.
- The EIS technique was useful for characterizing the resistance against corrosion of electrogalvanised steel samples coated with different conversion treatments. The number of time constants deconvoluted from the impedance spectra corresponding to each sample confirmed the protective action of the conversion layer containing Cr(III).
- The analysis and interpretation of all the experimental data showed that when the alternative conversion layer is sealed, their protective properties tend to improve although, in some cases, such effect may not be significant. Nevertheless, before a conclusive opinion can be inferred, it is necessary to test replicates of all the samples under different exposure conditions after being coated with specifically developed protective painting systems.

Acknowledgements

This research was financed by FAPERJ (Process E-26/152.259/2003), FINEP (Process no. 22.01.0752.00) of Brazil, and Comisión de Investigaciones Científicas de la Provincia de Buenos Aires (CIC) and Consejo Nacional de Investigaciones Científicas y Técnicas (CONICET) of Argentina. The authors are also grateful to IPT, Brazil, for the samples preparation.

References

[1] N. Zaki, Met. Finish. 86 (1988) 75–76.
[2] C. Gabrielli, M. Keddam, F. Minoutlet-Laurent, K. Ogle, H. Perrot, Electrochim. Acta 48 (2003) 965–976.

[3] A. Nazarov, D. Thierry, T. Prosek, N. Le Bozec, J. Electrochem. Soc. 152 (2005) B220–B227.
[4] P. Heffer, B. Lee, Steel Times Int. (January) (2005) 18–20.
[5] Definitions Committee, Federation of Societies for Coatings Technology, 1978, Philadelphia, p. 177.
[6] O. Bauer, O. Vogel, Int. Z. F. Metallogr. 8 (1916) 101.
[7] L.F.G. Williams, Plating (1972) 931.
[8] K.A. Korinek, ASM Handbook, vol. 13, ASM International, 1987.
[9] J. Bibber, Met. Finish. (February) (2002) 98.
[10] T. Bellezze, G. Roventi, R. Fratessi, Surf. Coat. Technol. 155 (2002) 221.
[11] C.S. Jeffcoate, H.S. Isaacs, A.J. Aldykiewicz Jr., M.P. Ryan, J. Electrochem. Soc. 147 (2000) 540.
[12] M. Kendig, S. Jeanjaquet, R. Addison, J. Waldrop, Surf. Coat. Technol. 140 (2001) 58.
[13] L. Xia, E. Akiyama, G. Frankel, R.L. McCreery, J. Electrochem. Soc. 147 (2000) 2556.
[14] J. Zhao, L. Xia, A. Sehgal, D. Lu, R.L. McCreery, G.S. Frankel, Surf. Coat. Technol. 140 (2001) 51.
[15] A. Boukamp, Equivalent Circuit, University of Twente, The Netherlands, 1989, Report CT88/265/128, CT89/214/128.
[16] G. Von Katen, Galvanotechnik 90 (1999) 650.
[17] R. Fratesi, G. Roventi, C.R. Tomachuk, J. Appl. Electrochem. 27 (1997) 1088.
[18] X. Zhang, C. van den Bos, W.G. Sloof, A. Hovestad, H. Terryn, J.H.W. de Wit, Surf. Coat. Technol. 199 (2005) 92.
[19] F. Mansfeld, J. Appl. Electrochem. 25 (1995) 187.
[20] F. Deflorian, S. Rossi, L. Fedrizzi, P.L. Bonora, Prog. Org. Coat. 52 (2005) 271.
[21] L. Fedrizzi, L. Claghl, B.L. Bonora, R. Fratessi, G. Riventi, J. Appl. Electrochem. 22 (1992) 247.
[22] C.M. Rangel, L.F. Cruz, Corros. Sci. 33 (1992) 1479.
[23] C. Cachet, R. Wiart, J. Electroanal. Chem. 111 (1980) 235;
C. Cachet, R. Wiart, J. Electroanal. Chem. 129 (1981) 103.
[24] A. Amirudin, D. Thierry, Prog. Org. Coat. 26 (1995) 1.
[25] C.M. Abreu, M. Izquierdo, M. Keddam, X.R. Nóvoa, H. Takenouti, Electrochim. Acta 41 (1996) 2401.
[26] B. del Amo, L. Véleva, A.R. Di Sarli, C.I. Elsner, Prog. Org. Coat. 50 (2004) 179.
[27] E.P.M. van Westing, G.M. Ferrari, F.M. Geenen, J.H.W. de Wit, Prog. Org. Coat. 23 (1993) 89.